Med Electron Microsc (2000) 33:217–230

ORIGINAL PAPER

**Li-Hua Tao · Hideaki Enzan · Yoshihiro Hayashi
Eriko Miyazaki · Toshiji Saibara · Makoto Hiroi
Makoto Toi · Naoto Kuroda · Keisi Naruse · Yu-Lan Jin
Li-Mei Guo**

Appearance of denuded hepatic stellate cells and their subsequent myofibroblast-like transformation during the early stage of biliary fibrosis in the rat

Received: October 12, 2000 / Accepted: 16 November, 2000

Abstract To investigate the early in vivo response of hepatic stellate cells in biliary fibrosis, we examined rat livers during the first 7 days after bile duct ligation using light microscopy, immunohistochemistry, electron microscopy, and immunoelectron microscopy. At day 1 after bile duct ligation, α-smooth muscle actin-positive fibroblasts appeared and then increased in number around the proliferating bile ductules. With time, the destruction of the external limiting plate became accentuated because of the invasion of the proliferating bile ductules and periductural fibrosis. At day 7, stromal cells containing fat droplets appeared in the fibrous tissue adjacent to the periportal parenchyma; these are termed denuded hepatic stellate cells. In the fibrous tissue disconnected from the liver parenchyma, the denuded hepatic stellate cells were replaced by myofibroblast-like cells. Meanwhile, the expression of transforming growth factor-β_1 on biliary epithelial cells increased. These results indicate the dual origin of myofibroblasts in experimental biliary fibrosis, the periductural and periductal fibroblasts in the initial stage, and the denuded hepatic stellate cells in the subsequent stage. These two types of stromal cells may undergo myofibroblastic transformation by the transforming growth factor-β_1 secreted by the proliferating biliary epithelial cells.

Key words α-Smooth muscle actin · Transforming growth factor-β_1 · Bile ductule · Bile duct ligation · Immunohistochemistry

L.-H. Tao · H. Enzan (✉) · Y. Hayashi · E. Miyazaki · M. Hiroi · M. Toi · N. Kuroda · K. Naruse · Y.-L. Jin · L.-M. Guo
First Department of Pathology, Kochi Medical School, Kohasu, Okocho, Nankoku, Kochi 783-8505, Japan
Tel. +81-88-880-2329; Fax +81-88-880-2332
e-mail: enzanh@kochi-ms.ac.jp

T. Saibara
First Department of Internal Medicine, Kochi Medical School, Kochi, Japan

Introduction

Liver fibrosis is a common response to various chronic liver injuries.[1] Previous studies on liver fibrosis in human and experimental animals clarified that hepatic stellate cells (HSCs) (Ito cells, fat-storing cells, lipocytes) adjacent to necrotic liver cells promptly proliferate and undergo phenotypic modulation toward myofibroblast-like cells.[2–10] The myofibroblastic transformation is induced by alterations of the neighboring extracellular matrix,[2] the action of humoral factors derived from necrotic liver cells,[11] and cytokines,[1–4,7,10–13] particularly transforming growth factor-β_1 (TGF-β_1),[9,14–16] secreted by Kupffer cells, sinusoidal endothelial cells, platelets, infiltrating inflammatory cells, and activated HSCs themselves.[4,7,9,12,14,16] So long as the necroinflammatory injuries continue, the transformed HSCs actively produce various components of the extracelluar matrix, resulting in new fiber formation in the injured sites. Therefore, the activated HSCs with myofibroblastic phenotypes are the principal effector cells in liver fibrogenesis.[1,4,9,17]

On the other hand, biliary fibrosis is considerably different from other types of liver fibrosis following liver cell necrosis.[18–20] It is always associated with rapid extensive bile duct proliferation,[18–20] but with little necrosis and inflammatory reaction.[19–21] The proliferating biliary epithelial cells themselves promote fibrogenesis by a number of mechanisms, including the production of cytokines, such as TGF-β_1,[22] platelet-derived growth factor (PDGF) -BB,[23] and neutrophil chemoattractants.[24] Subsequently, biliary fibrosis develops exclusively from the portal tracts, in close association with proliferating bile ductules.[18,19,25] Experimental studies of liver injuries induced by ligation of the common bile duct (CBD), a model for biliary fibrosis, showed that portal fibroblasts differentiated toward myofibroblasts and then participated in the development of fibrosis.[26–28]

Maher et al.[17] suggested, by quantitating the relative abundance of specific mRNA for collagen types I, III, and IV and laminin in each purified liver cell population from

normal and CBD-ligated rat livers, that HSCs were important effectors in the early stage of biliary fibrosis. Furthermore, Milani et al.[15] showed, in studying procollagen gene expression at the level of RNA transcripts by in situ hybridization, that HSCs and transitional cells were responsible for the excessive collagen deposition in advanced biliary fibrosis. However, when the external limiting plate remains intact, biliary fibrosis is predominantly localized around the proliferating bile ductules in the portal tracts. Then, following the disruption of the external limiting plate by the progression of biliary fibrosis, periportal and septal fibrosis are superimposed. A prolonged bile duct obstruction finally leads to biliary cirrhosis.[7,29] Thus, it is reasonable to classify biliary fibrosis into two stages: concentric periductural fibrosis around the proliferating bile ductules in the initial stage for a very short duration and the additional periportal and septal fibrosis in the later, longer stage.

The aim of this study was to identify which types of cells are the most effective for excessive production of the extracellular matrix components at each stage of biliary fibrosis and also to investigate how and where the cells transform to myofibroblasts.

Materials and methods

Animals

Seventy-six male Wistar strain rats (SLC, Hamamatsu, Japan) weighing 200–225 g, were used in this study. The animals had free access to water and food and were maintained in a constant laboratory environment with respect to temperature, humidity, and daylight cycle. Fifty-six rats were laparotomized under anesthesia (Nembutal; Dainabot, North Chicago, IL, USA; 50 mg/kg body weight, intraperitoneally). In half of them, the common bile duct (CBD) was exposed and carefully ligated with a silk thread. The other half underwent laparotomy, but no CBD ligation was performed (sham-operated rats).

After the operations, all 56 rats were returned to the laboratory. In the following week, from day 1 to day 7 after operation, 4 CBD-ligated rats and 4 sham-operated rats per day, respectively, were killed under anesthesia. Four unoperated rats, which served as normal controls, were also kept under the same laboratory environment.

For the determination of total bilirubin, peripheral blood samples were collected from 16 other rats at 1, 4, and 7 days after CBD ligation and also from normal rats, 4 rats in each group. The blood samples were centrifuged (300 g, 10 min) and were measured by standard methods. This study was approved by the Animal Care and Use Committee of Kochi Medical School and followed the National Institutes of Health guidelines for the humane care and use of animals.

Light microscopy

Liver tissues were removed under light ether anesthesia of the rats, fixed in 10% neutral buffered formalin for 2 days, and then embedded in paraffin. Sections cut at 4 μm in thickness were stained with hematoxylin and eosin, with silver impregnation for reticular fibers and with Azan staining for collagen fibers.

Immunohistochemistry

The sections of periodate-lysine-paraformaldehyde (PLP) - fixed and paraffin-embedded liver tissue were deparaffinized and rehydrated. Endogenous peroxidase was inhibited with 0.3% hydrogen peroxide in methanol for 5 min at room temperature and rinsed with phosphate-buffered saline (PBS, pH 7.4) (5 min, 2 times), and incubated in 10% normal rabbit serum for 10 min for immunostaining of the monoclonal antibodies listed in Table 1. The same procedure using 10% normal swine serum was performed for immunostaining of the polyclonal antibody against transforming growth factor-β_1 (TGF-β_1) (Table 1). Subsequently, they were incubated overnight at 4°C. After rinsing with 0.01 M PBS, the sections were incubated for 1 h at room temperature with a 1:200 dilution of biotinylated rabbit antimouse IgG $F(ab')^2$ fragment (DAKO, Glostrup, Denmark) for monoclonal antibodies and a 1:200 dilution of biotinylated swine anti-rabbit IgG $F(ab')^2$ fragment (DAKO) for TGF-β_1. After rinsing with PBS, these sections were incubated for 1 h at room temperature in an avidin-biotin-peroxidase complex (ABC) solution. The ABC components were obtained in kit form (Vectorstain; ABC Kits, Vector, Burlingame, CA, USA). Finally, the sections were immersed in a substrate solution of 0.5% 3,3′-diaminobenzidine tetrahydrochloride (Sigma, St. Louis, MO, USA) and 0.1% hydrogen peroxide in 0.05 M Tris buffer, pH 7.6, for 3 min at room temperature, washed lightly, counterstained with hematoxylin, dehydrated in ethanol, and mounted with Eukitt (Kindler, Freiburg, Germany). As a negative control for immunostaining,

Table 1. Antibodies used for immunohistochemical analysis

Antibodies (clone)	Specificity	Source	Working dilution	Antigen retrieval
Monoclonal				
(1A4)	α-smooth muscle actin	DAKO, Glostrup, Denmark	1:50	Not performed
(PC10)	Proliferating cell nuclear antigen	DAKO, Glostrup, Denmark	1:10	Not performed
(ED1)	Rat monocytes and macrophages	Serotec, Oxford, England	1:100	0.1% Pronase E
Polyclonal	Transforming growth- factor-β1	Promega, Madison, WI, USA	1:50	0.1% Pronase E

All antibodies were diluted in phosphate-buffered saline (PBS, pH 7.4)

sections were incubated in normal mouse or rabbit serum at the same concentration as that of the primary antibodies.

Electron and immunoelectron microscopy

Small pieces of liver tissue were prefixed in 2.5% glutaraldehyde in 0.1 M phosphate buffer (PB, pH 7.4) for 24 h at 4°C and postfixed in 1% osmium tetroxide in PB for 2 h at 4°C, followed by dehydration and embedding in epoxy resin. For selecting optimal areas for this study, semithin sections were stained with toluidine blue. Ultrathin sections stained with uranyl acetate and lead citrate were examined with an electron microscope (JEM-100S; JEOL, Tokyo, Japan). Other pieces of liver tissue were fixed in PLP solution for 18 h at 4°C. Tissue sections were cut 50 μm thick using a microslicer (DTK-2000; D.S.K., Kyoto, Japan) and washed in cold PBS, followed by incubation for 18 h at 4°C in PBS containing a 1:50 dilution of anti-α-smooth muscle actin (anti-ASMA) and anti-TGF-β_1. The sections were incubated in an ABC solution. Then, the conventional procedures for immunohistochemistry and electron microscopy as described earlier were performed.

Results

Blood chemical examination

The serum level of total bilirubin linearly rose until day 4, showing the rapid development of extrahepatic cholestasis. The level of bilirubin then decreased, but remained at a high level by day 7 after CBD ligation (Table 2).

Light microscopic and immunohistochemical observations

In the nontreated control rats (Fig. 1), Azan staining and silver impregnation showed a very small amount of both collagen and reticular fibers around the central veins and in the small portal tracts (Fig. 1a). The large portal tracts contained more abundant fibrous stroma in which mast cells were occasionally scattered. Immunoreactivity for ASMA was only detected in the walls of the blood vessels (Fig. 1b). In the portal tracts and around the bile ducts/ductules, there were a few spindle-shaped fibroblasts that were generally negative for ASMA. Only a few hepatocytes and biliary epithelial cells were positive for proliferating cell nuclear antigen (PCNA) (Fig. 1c). The bile duct epithelium stained weakly positive for TGF-β_1 whereas the liver cells stained negative (Fig. 1d). The HSCs were readily recognized along the sinusoidal wall in the glutaraldehyde and osmium tetroxide-fixed, epoxy resin-embedded sections stained with toluidine blue. An outstanding characteristic of the cells was the presence of several intracytoplasmic fat droplets, up to 3 μm in diameter. In the sham-operated rats, hepatic morphology was normal at each day after operation.

In the CBD-ligated rats (Figs. 2–4), on the first day after ligation mild proliferation of marginal bile ductules was seen in the portal tracts, which were slightly edematous. Azan staining and silver impregnation showed an increase of both collagen and reticular fibers around the proliferating bile ductules (Fig. 2a). A few ASMA-positive fibroblasts appeared around the bile ductules and ducts at the early stage (Fig. 2b, inset) when the outer limiting plates remained intact. At day 2 after CBD ligation, the ASMA-positive fibroblasts increased in number (Fig. 2b) and then circumferentially covered the proliferating bile ductules. However, no increased expression of ASMA was seen in the adjacent parenchyma (Figs. 3b, 4b).

From day 2 on, the external limiting plates became focally depressed or destroyed because of the budlike invasion of the proliferating bile ductules into the periportal parenchyma. These changes gradually increased by day 7 after operation. At this time, the proliferating bile ductules together with the concentric fibrosis around them significantly extended from the periportal areas into the neighboring parenchyma, resulting in irregular extension and widening of the portal tracts.

Almost all the nuclei of the biliary epithelial cells were positive for PCNA (Figs. 2c, 3c, 4c). PCNA-positive stromal cells were scattered in areas of new fiber formation (Fig. 4c, inset). The intensity of TGF-β_1 immunoreactivity on the biliary epithelial cells and mast cells was increased in association with the progression of biliary fibrosis (Figs. 2d, 3d, 4d). An inflammatory cell infiltration largely consisting of lymphocytes, neutrophils, and ED1-positive macrophages became more numerous with time in the areas of periductural and perilobular fibrosis (Fig. 5a,b).

Electron and immunoelectron microscopic observations

In the nontreated control rats, the fibroblasts of the portal tracts possessed scanty cytoplasm and contained a few small mitochondria and poorly developed rough-surfaced endoplasmic reticulum. In these cells, small fat droplets were generally absent. Irregularly shaped, short segments of thin cytoplasmic processes of the fibroblasts were seen. The

Table 2. Blood chemistry

Parameter	Control rats (n = 4)	CBD-ligated rats (n = 4 in each group)		
		1 day	4 days	7 days
Total serum bilirubin (mg/dl)	0.28 ± 0.17	4.15 ± 0.24	8.73 ± 6.12	5.70 ± 1.05

CBD, common bile duct
Values are mean ± SD

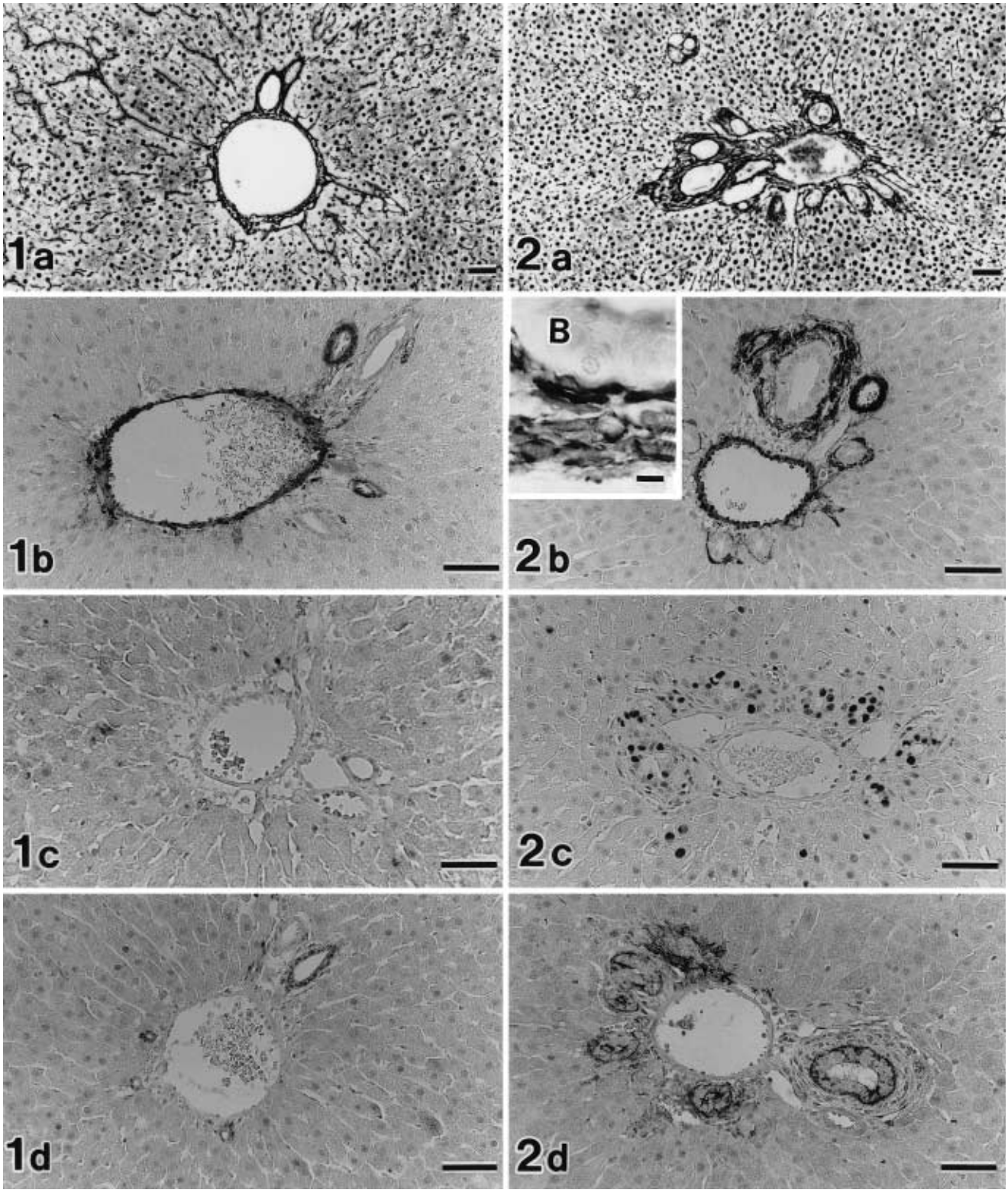

Fig. 1a–d. Portal tracts and periportal parenchyma of control rat liver tissue. **a** Small amounts of reticular fibers are observed in the portal tract. **b** α-smooth muscle actin (ASMA) expression is restricted to the vessel walls. **c** Only a few biliary epithelial cells and liver cells are positive for proliferating cell nuclear antigen (PCNA). **d** The biliary epithelial cells stain weakly positive for transforming growth factor-β_1 (TGF-β_1)

Fig. 2a–d. Portal tracts and periportal parenchyma of liver tissue of rats at day 2. With time after operation, the reticular fibers increase in volume around the proliferating bile ductules. The extension of the proliferating bile ductules into the periportal parenchyma and the focal destruction of the limited plates are frequently seen (**a**). ASMA-positive stromal cells appear around proliferating bile ductules (**b** *inset*; *B*, bile ductule; *bar*, 5 μm) and increase in number throughout the enlarged portal tract. However, there is no staining for ASMA in the lobules (**b**). Almost all the proliferating biliary epithelial cells show positive reaction for PCNA (**c**). TGF-β_1 expression in the proliferating biliary epithelial cells is increased with time after operation (**d**). *Bar,* 50 μm; **a** Reticulin stain; **b–d** Immunostaining for ASMA, PCNA, and TGF-β_1

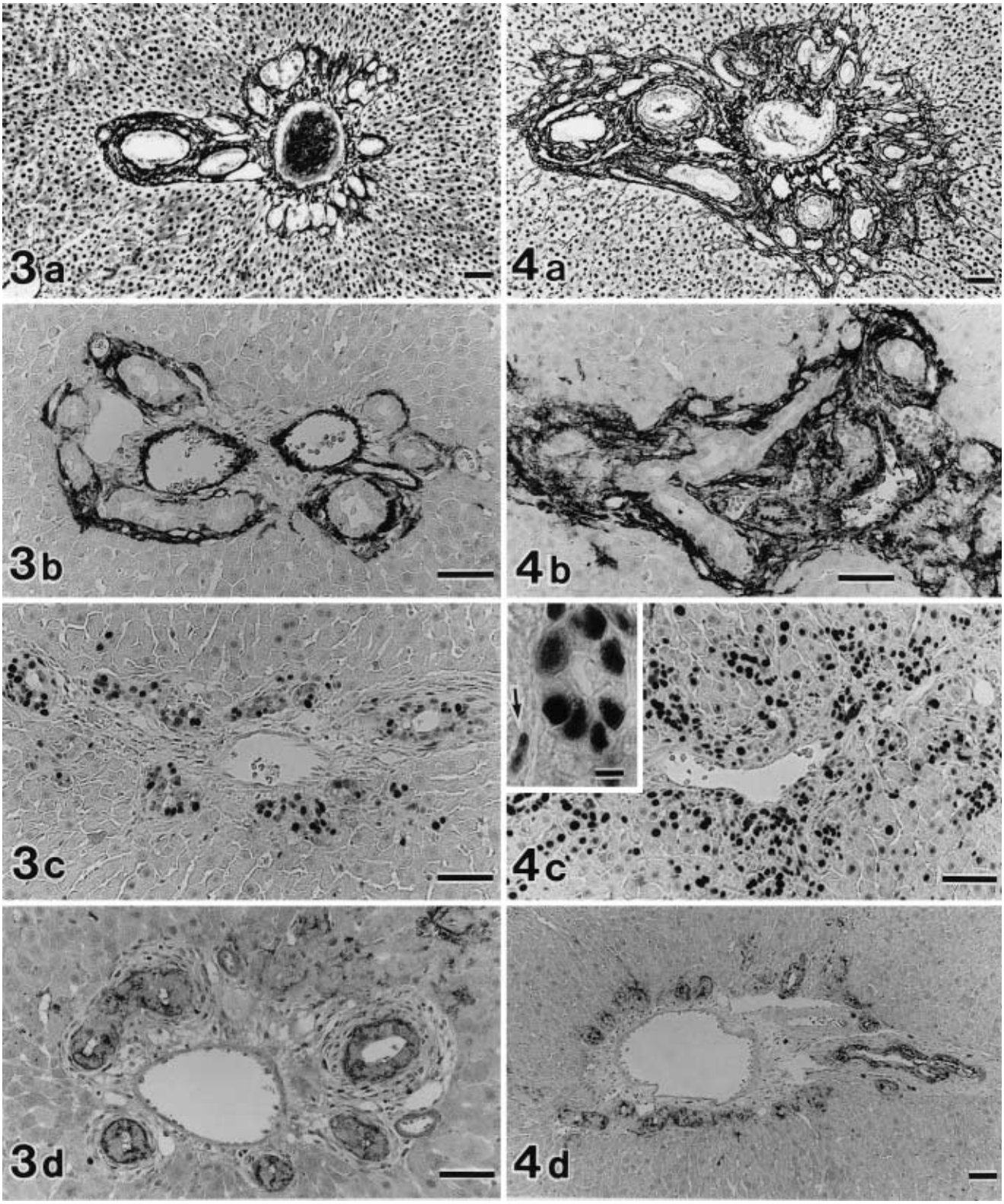

Fig. 3a–d. Portal tracts and periportal parenchyma of liver tissue of rats at day 4. Description of figure parts, magnification, and staining same as Fig. 2 except for inset

Fig. 4a–d. Portal tracts and periportal parenchyma of liver tissue of rats at day 7. Description of figure parts, magnification, and staining same as Fig. 2 except for inset. A PCNA-positive stromal cell (**c** *inset*; *arrow*; *bar*, 5 μm) is seen in the periductural fibrous tissue

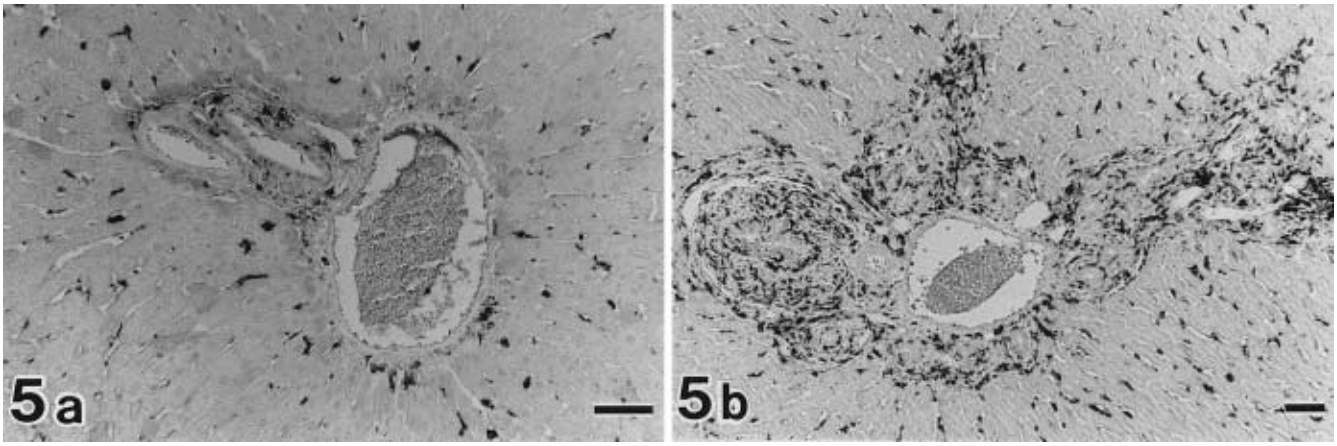

Fig. 5a,b. Immunostaining on sections of rat livers with an antibody against ED-1, a monoclonal antibody specific for rat monocytes and macrophages. **a** In a control rat liver, ED-1-positive macrophages are distributed in a scattered fashion along the sinusoidal walls. **b** At day 7 after CBD ligation, ED-1-positive macrophages have intensely infiltrated the enlarged portal tract. The number of sinusoidal macrophages has also increased. *Bar* 50 μm

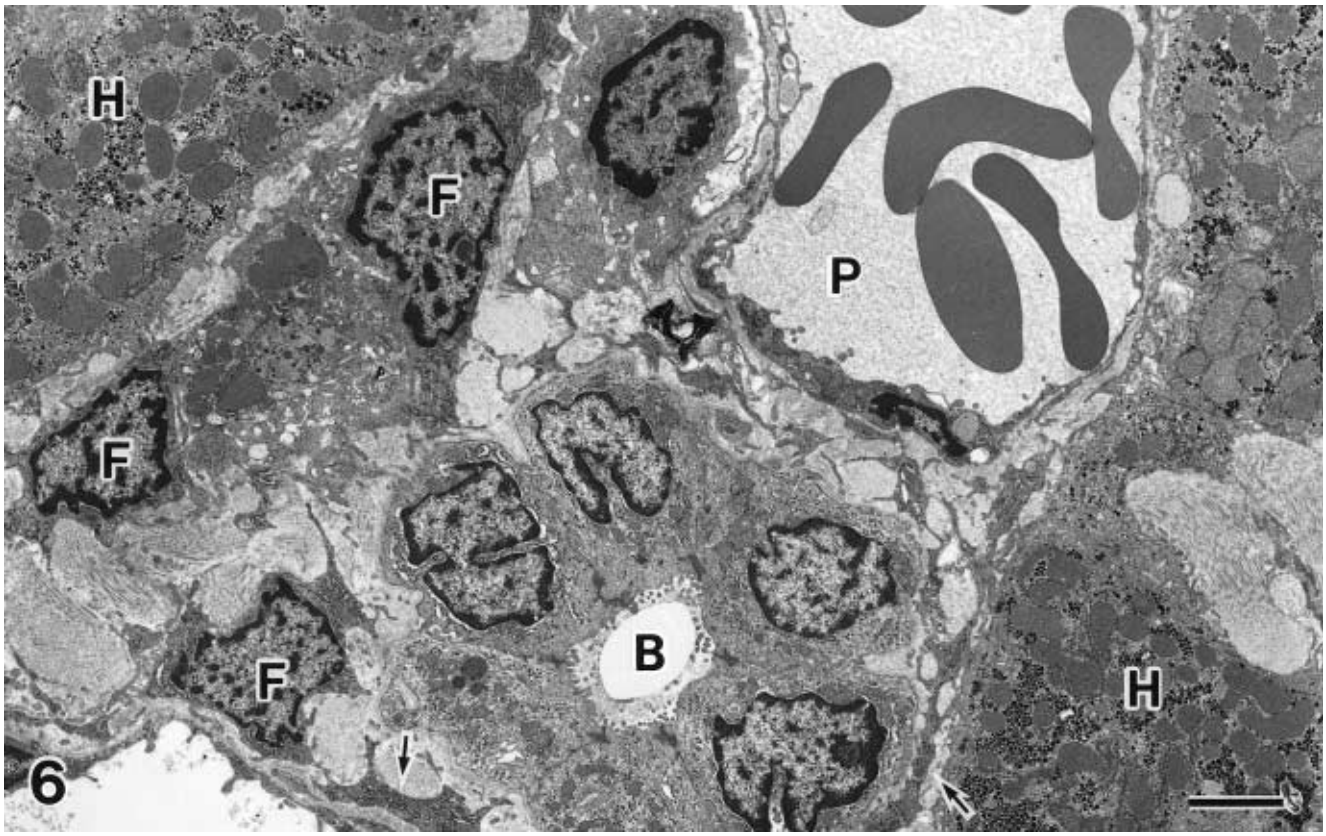

Fig. 6. Electron photomicrograph of a portal tract in the control rat. The portal fibroblasts (*F*) extend the cytoplasmic processes (*arrow*) around a bile duct (*B*). *H*, hepatocyte; *P*, portal vein. *Bar* 20 μm

extracellular matrix of the portal tracts was composed of small amounts of amorphous materials and a few collagen fibrils (Fig. 6). Compared with hepatocytes, the cuboidal to columnar biliary epithelial cells contained smaller amounts of cell organelles. In the periphery of the liver lobules, hepatic stellate cells (HSCs) were evenly distributed. Their cytoplasmic organelles were inconspicuous except for several small fat droplets.

In the CBD-ligated rats, the proliferating bile ductules contained more polyribosomes and rough-surfaced endoplasmic reticulum compared with those in the normal control rats. ASMA-positive periductural fibroblasts had

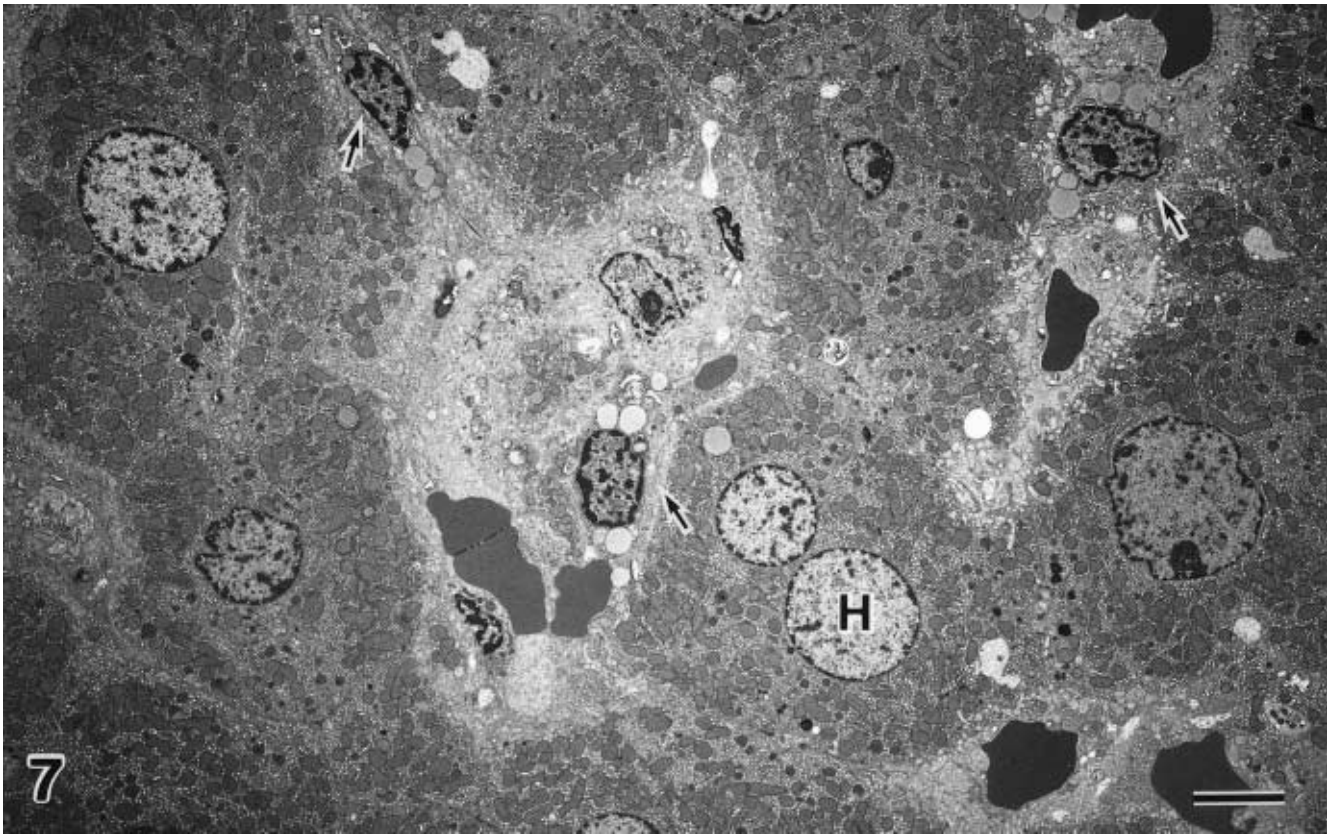

Fig. 7. Quiescent hepatic stellate cells (HSCs) in zone 1 of the liver parenchyma show a tendency to clump at day 1 after CBD ligation. *H*, hepatocyte; *arrow*, quiescent HSC containing several small fat droplets. *Bar* 5 μm

numerous and slightly dilated rough-surfaced endoplasmic reticulum. The quiescent HSCs in zone 1 took an approximate position with each other and appeared to gather in that location (Fig. 7). Where proliferating bile ductules with periductular fibrosis extended into the periportal parenchyma, the invading bile ductules contacted directly with the HSCs (Fig. 8). At day 7 after CBD ligation, when biliary fibrosis was most advanced in this study, the quiescent HSCs focally accumulated in the periportal parenchyma adjacent to periportal fibrosis (Fig. 9). In contrast, in the fibrous tissue immediately adjacent to the parenchyma, stromal cells containing small fat droplets, as do quiescent HSCs, were frequently found (Fig. 10a–d). They were all negative for ASMA.

Around these HSC-like stromal cells, however, neither liver cell plates nor sinusoidal structures were present. In the fibrous tissue disconnected from the parenchyma, the HSC-like stromal cells were replaced by myofibroblast-like cells or transitional cells. These stromal cells revealed the ultrastructural features of the myofibroblasts, i.e., the absence of fat droplets, the presence of well-developed rough-surfaced endoplasmic reticulum, and large Golgi complexes. An increased number of microfilaments underneath the plasma membrane were correlated with the strong immunohistochemical reaction for anti-ASMA antibody (Fig. 11). The ASMA-positive myofibroblast-like or transitional stromal cells were closely contacted with numerous collagen fibrils, infiltrating inflammatory cells, and the proliferating bile ductules. In the cytoplasm of the biliary epithelial cells, the electron-dense products of TGF-β_1 were predominantly seen on the rough-surfaced endoplasmic reticulum (Fig. 12).

In addition, the negative control sections for immunohistochemistry constantly displayed a negative reaction.

Discussion

We demonstrated in this study the very early occurrence of periductular fibrosis and then progressive periportal fibrosis over a 7-day period after CBD ligation. The development of fibrosis was closely associated with the phenotypic changes of both periductural and periductal fibroblasts and quiescent HSCs toward myofibroblast-like cells. Previous studies have strongly suggested that activation of HSCs was the initial and critical event in the development of liver fibrosis, regardless of etiology.[1,9,10,30] The myofibroblastic transformation of HSCs is easily identified by their strong immunohistochemical expression of ASMA.[5,6,8] The initial changes after CBD ligation, however, appeared to be predominantly confined to the portal tracts, while the liver parenchyma was relatively well preserved.

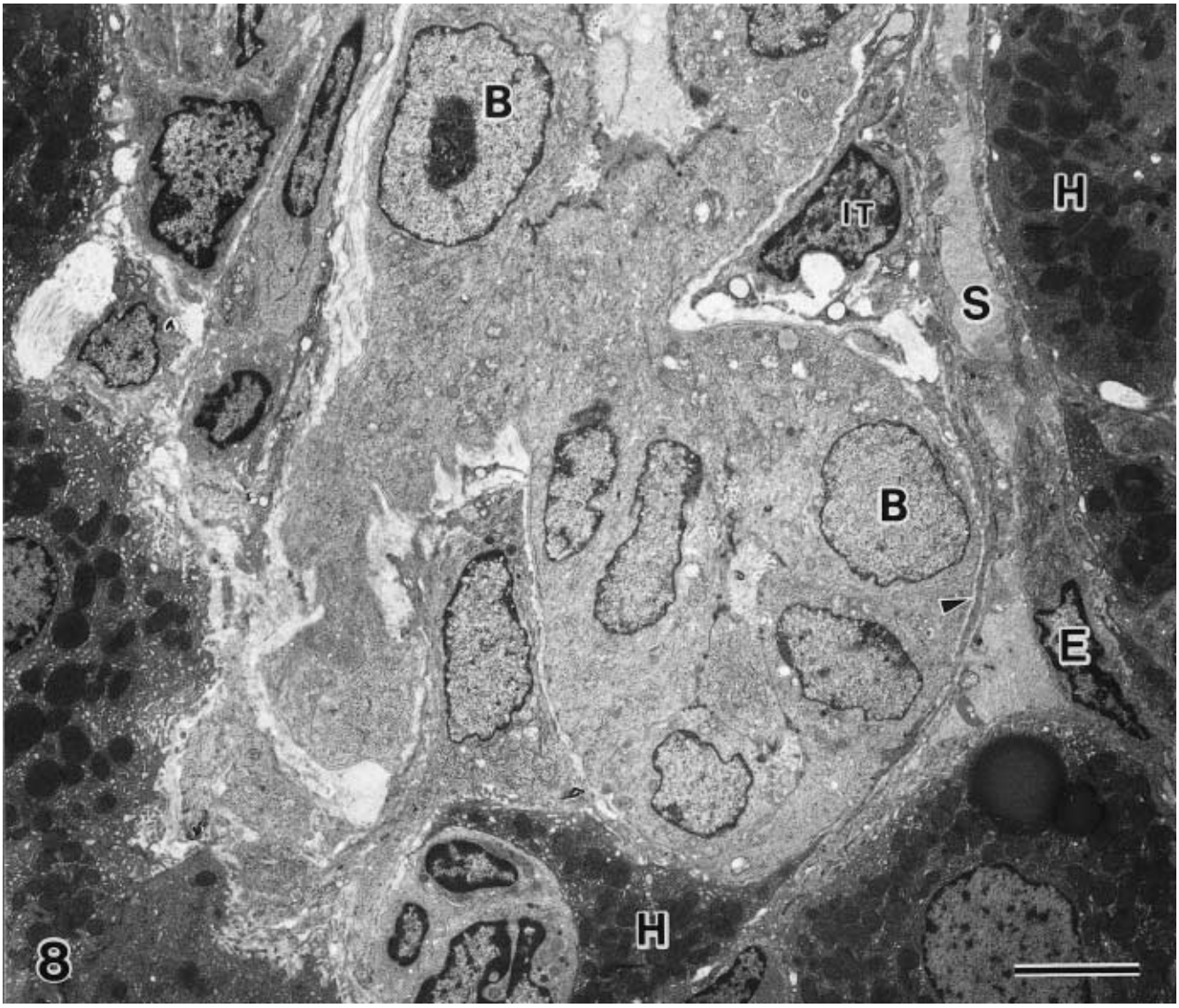

Fig. 8. Direct contact of the proliferating biliary epithelial cell with a residual HSC at day 2 after CBD ligation. Around the HSC (*IT*), the liver cell–sinusoid structure is partially lost. *B*, proliferating biliary epithelial cell; *E*, sinusoidal endothelial cell; *H*, hepatocyte; *S*, sinusoid; *arrowhead*, cytoplasmic process of the HSC. *Bar* 5 μm

In normal rats, quiescent HSCs are located underneath the endothelial lining in the space of Disse and are distributed at random at certain distances. Periductural fibroblasts are very few in number and negative for ASMA. However, as early as day 1 after CBD ligation, periductular fibroblasts became positive for ASMA, showing their phenotypic modulation toward myofibroblast-like cells. Considering these findings together with the subsequent development of periductural fibrosis, periductular fibroblasts may participate in the very early stage of biliary fibrosis, which is in agreement with a previous report.[27] Parallel to the development of periductular fibrosis, the ASMA-positive periductular fibroblasts increased in number. This may be, at least in part, the result of the local proliferation of portal fibroblasts and their phenotypic modulation, as reported by previous studies.[7,26,27]

On the other hand, with time after CBD ligation, especially at day 7 after operation in this study, the increased invasion of proliferating bile ductules with periductular fibrosis into the liver parenchyma caused a frequent appearance of small fat droplet-containing stromal cells in the loose fibrous tissue immediately adjacent to the liver parenchyma. Although these cells completely lost the topographical relationship to liver cells and sinusoids, they showed the same morphological features as quiescent HSCs, i.e., the presence of several small intracytoplasmic fat droplets. Figure 10a–c shows that these cells derive from the quiescent HSCs in the periportal zone of the liver parenchyma; they are termed denuded HSCs in the perilobular loose fibrous tissue.

We herein report for the first time the appearance of denuded HSCs in the front of biliary fibrosis, namely at the

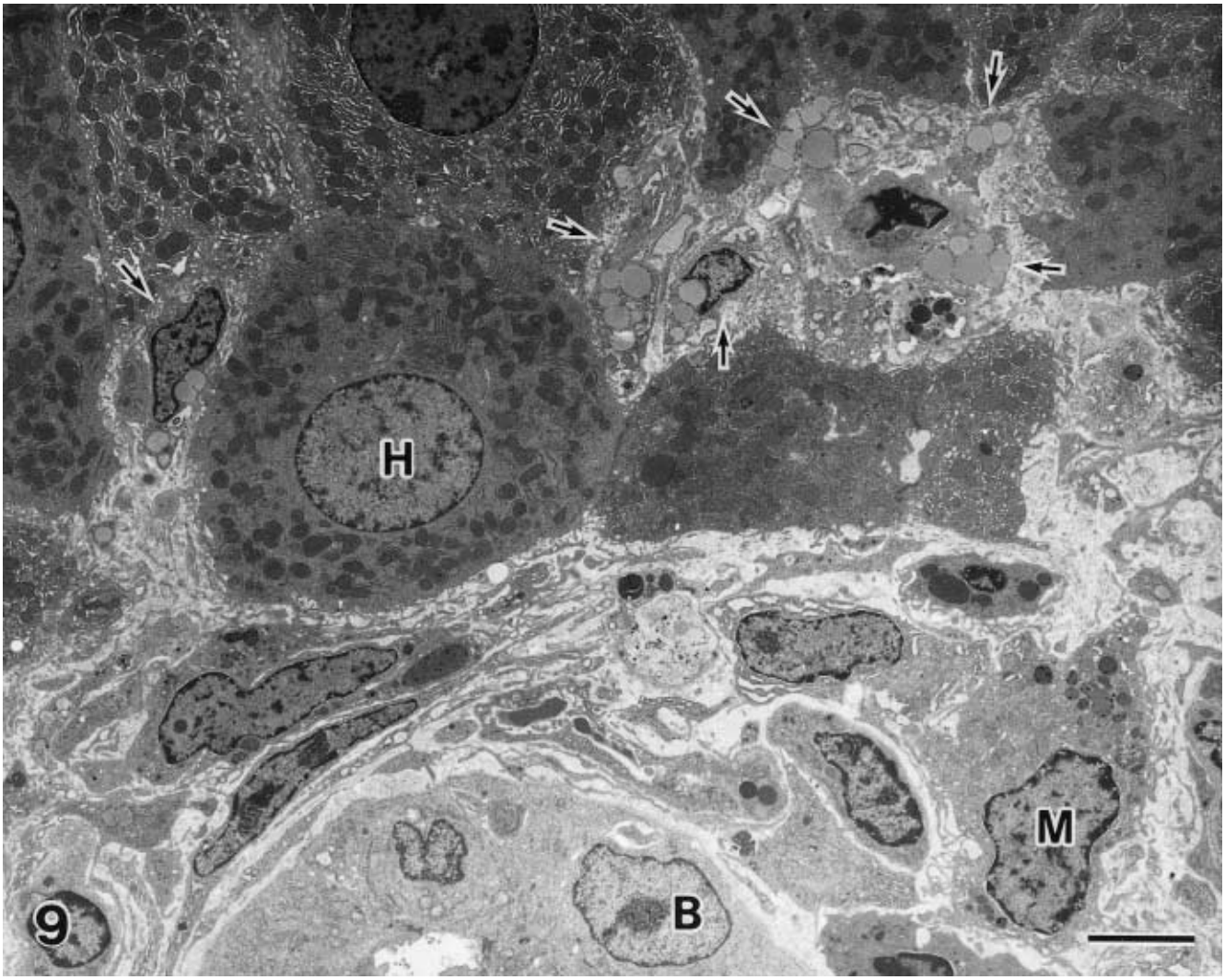

Fig. 9. Focal accumulation of quiescent HSCs in the periportal zone in close proximity to periportal fibrous tissue at day 7 after CBD ligation. *B*, bile duct; *H*, hepatocyte; *M*, macrophage; *arrows*, quiescent HSCs. *Bar* 5 μm

periportal fibrous tissue–parenchymal interface. The site of the denuded HSCs corresponded well to the location in which tenascin, a noncollagenous glycoprotein of the extracellular matrix playing a role in extracellular matrix organization and also in the migration of cells, was intensely expressed from day 7 onward after CBD ligation.[25]

Niiro et al.[31] reported that the limiting plates of hepatocytes separated the space of Disse from the portal tracts and lymphatics. The disruption of the limiting plates resulting from the invasion of the proliferating bile ductules into the periportal parenchyma may directly connect the space of Disse with the interstitial space of the portal tract. This may provide a migratory pathway for HSCs, even though HSCs in the quiescent stage, to move to the periportal areas, causing the local increase of quiescent HSCs. In the case of extrahepatic biliary obstruction, the number of HSCs and their fat droplets were considerably increased.[32]

Furthermore, experimental biliary fibrosis was accompanied by an increased number of periportal desmin-positive HSCs at the initial stage[7,33] and followed by a marked increase in number of desmin-positive and ASMA-positive stromal cells, considered myofibroblasts, in the areas of periductural fibrosis from day 7 onward after CBD ligation. The denuded HSCs, derived from the increased quiescent HSCs in the periportal zone, may play a major role in the recruitment of myofibroblast-like cells in biliary fibrosis. This study also showed that all the proliferating biliary epithelial cells stained strongly positive for TGF-β_1 and that a progressive upregulation of TGF-β_1 expression occurred with the progress of biliary fibrosis. Moreover, our immunoelectron microscopic investigation using the ABC method confirmed the predominant localization of TGF-β_1 on the rough-surfaced endoplasmic reticulum of the proliferating biliary epithelial cells.

It is well known that TGF-β_1 acts as a potent fibrogenic cytokine[9,14–16] and promotes the morphological and functional differentiation of stromal cells to myofibroblasts. Bissel et al.[16] reported that total TGF-β mRNA, including TGF-β_1, TGF-β_2, and TGF-β_3, was increased only in the cell

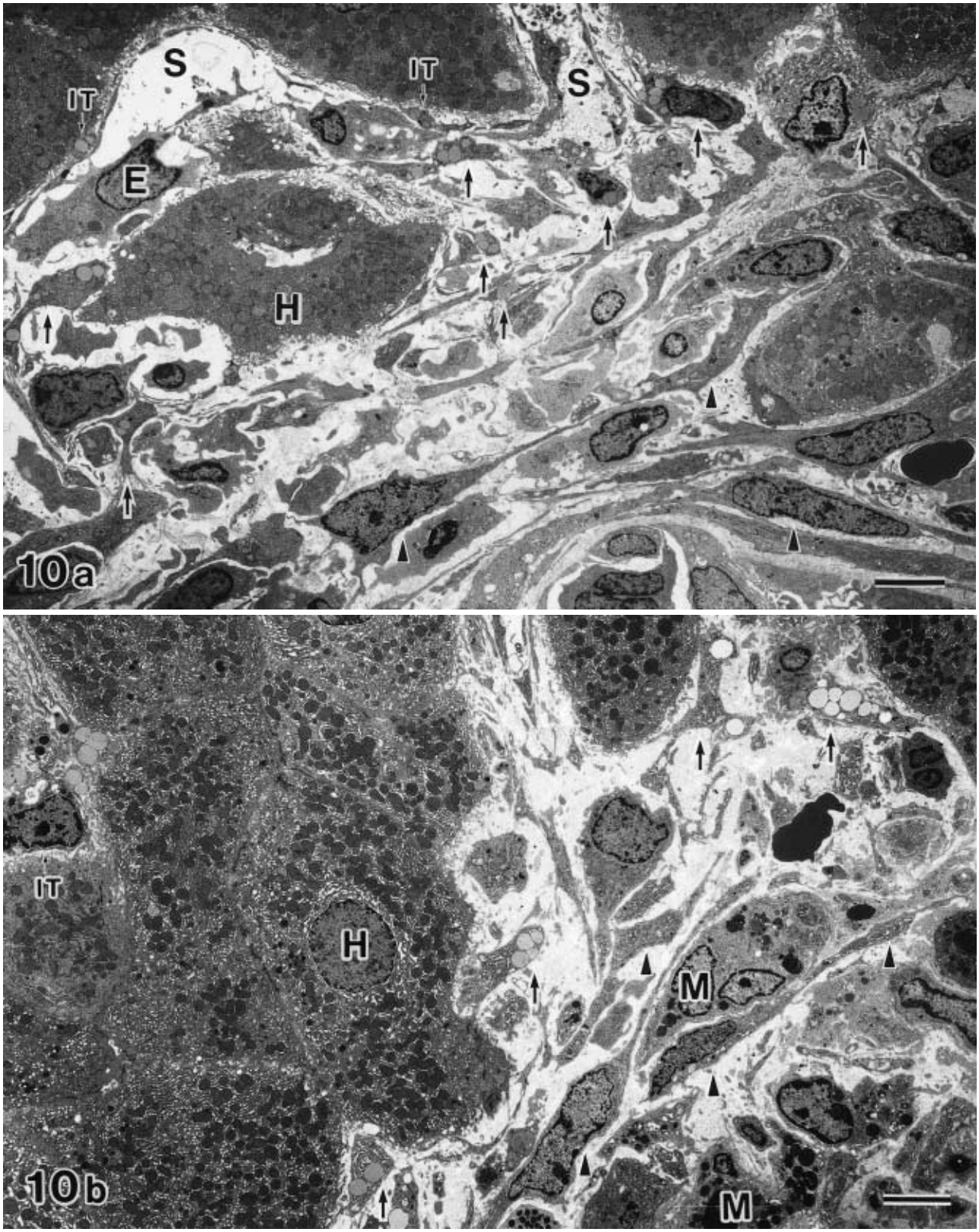

Fig. 10a–d. Electron photomicrographs of the denuded HSCs at day 7 after CBD ligation. HSCs generally appear in the fibrous tissue immediately adjacent to the liver parenchyma. Although the adjacent liver cell and sinusoidal structure are lost, they can be easily identified by the intracytoplasmic fat droplets, similar to those of quiescent HSCs (*IT*). In the fibrous tissue disconnected from the liver parenchyma, the myofibroblast-like cells (*arrowhead*) and transitional cells appear and are closely intermingled with infiltrating inflammatory cells (**a**,**b**) and proliferating bile ductules (**c**). **d** Higher magnification of quiescent HSCs (*IT*), denuded HSCs (*arrow*), and myofibroblast-like cells (*arrowhead*). *B*, proliferating bile ductule; *H*, liver cell; *L*, lymphocyte; *M*, macrophage; *S*, sinusoid; *arrow*, denuded HSCs. *Bars* 5 μm (**a–c**); 2.5 μm (**d**)

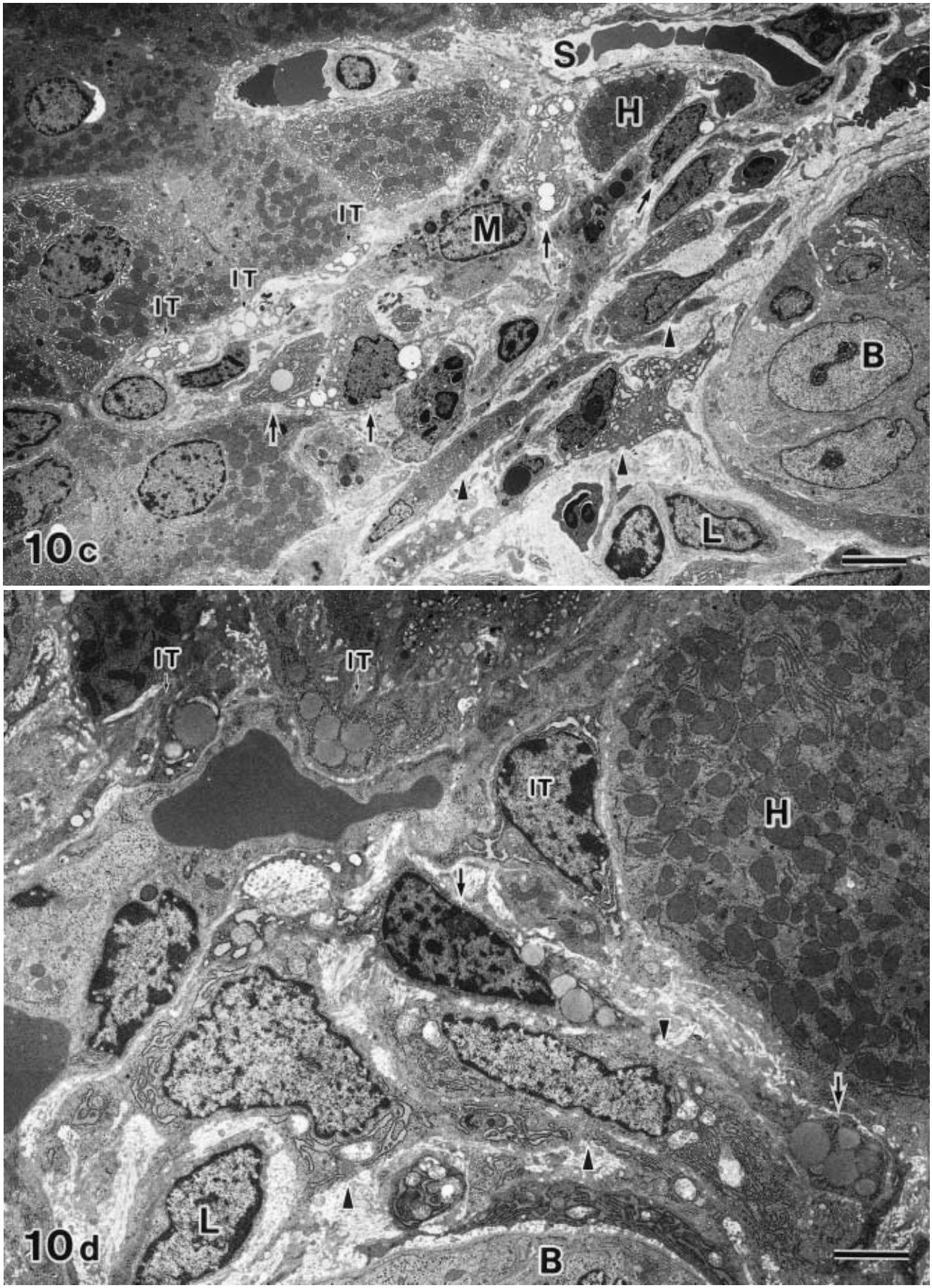

Fig. 10a–d. *continued*

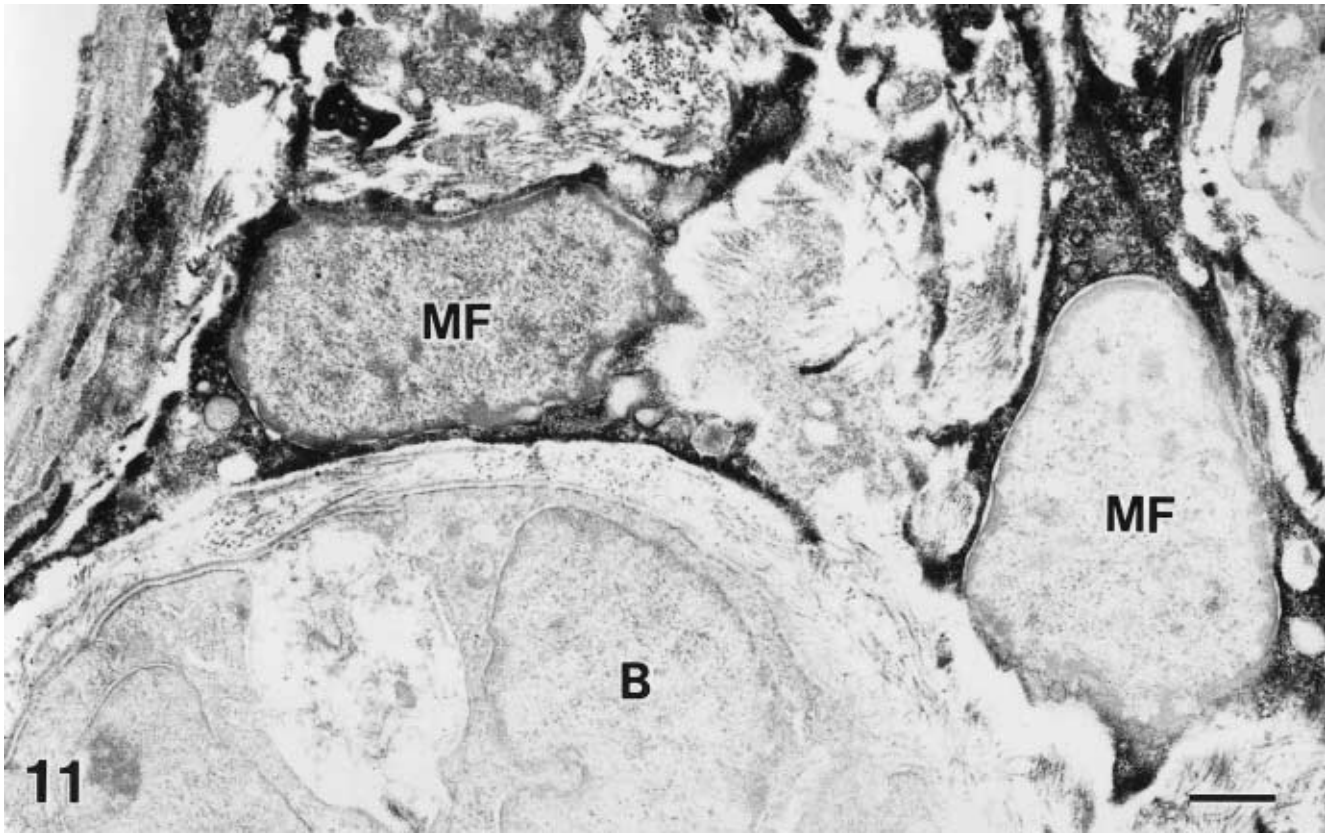

Fig. 11. Immunoelectron photomicrograph of periductural myofibroblast-like cells at day 7 after CBD ligation. Section incubated with anti-ASMA. ASMA-positive myofibroblast-like cells (*MF*) are seen around the bile ductule (*B*). *Bar* 1 μm

fraction of HSCs and that the increase was progressive over a 7-day period after CBD ligation, suggesting the autocrine regulation of TGF-β on the cells.

On the other hand, isolates of biliary cells expressed all three TGF-β subtypes at a relatively high level, similar to normal Kupffer cells. According to Milani et al.,[15] high TGF-β_2 levels were present only in the proliferating bile ductules of rat livers 3 weeks after CBD ligation, whereas TGF-β_1 mRNA was detected at high levels in most mesenchymal and inflammatory cells and in a few biliary epithelial cells. In patients with biliary atresia, TGF-β_1 mRNA expression was demonstrated in the bile duct epithelial cells, HSCs, and hepatocytes close to the fibrotic septa.[34] Saperstein et al.[35] reported that the expression of TGF-β_1 on rat biliary epithelial cells after CBD ligation may result primarily from an augmented uptake rather than from synthesis of this growth factor. On the other hand, PDGF[23] and monocyte chemotactic protein-1[36] have been recently identified as potent chemoattractants for HSCs. However, as TGF-β_1 has been known to regulate PDGF receptor β-subunit in HSCs,[37] TGF-β_1 secreted from proliferating biliary epithelial cells may also function to increase the migration of periportal quiescent HSCs and denuded HSCs to the periportal necroinflammatory lesions following the destruction of the external limiting plates.

Although the expression of TGF-β_1 in the proliferating bile ductules and its significance in biliary fibrosis remains unsettled, we have shown a possibility that TGF-β_1 produced by proliferating biliary epithelial cells mediates, through the effects of paracrine, not only the migration of the denuded HSCs but also their conversion to myofibroblasts. In the initial stage after CBD ligation, the periductural fibroblasts also may be transformed to myofibroblast-like cells in a similar way.

In conclusion, we demonstrated the dual origins of myofibroblasts in experimental biliary fibrosis: the periductural fibroblasts in the initial stage for a very short duration after CBD ligation; and the denuded HSCs in the subsequent stage for a longer duration after the destruction of the external limiting plates. The denuded Ito cells, derived from the increased quiescent HSCs in the periportal zone, appeared in the fibrous tissue at the fibrous tissue–parenchymal interface, following the destruction and loss of the adjacent liver cell–sinusoid structure caused by the invasion of the proliferating bile ductules with periductural fibrosis. Thereafter, through the paracrine effect of TGF-β_1 secreted by the biliary epithelial cells, the denuded HSCs may migrate and convert their phenotype toward myofibroblasts and predominantly participate in the later stages of biliary fibrosis.

Acknowledgments We gratefully acknowledge the technical assistance of Tadatoshi Tokaji, Hisayo Yamasaki, and Naoyo Nakamura. We also thank Dr. Hirofumi Nakayama and David Blake

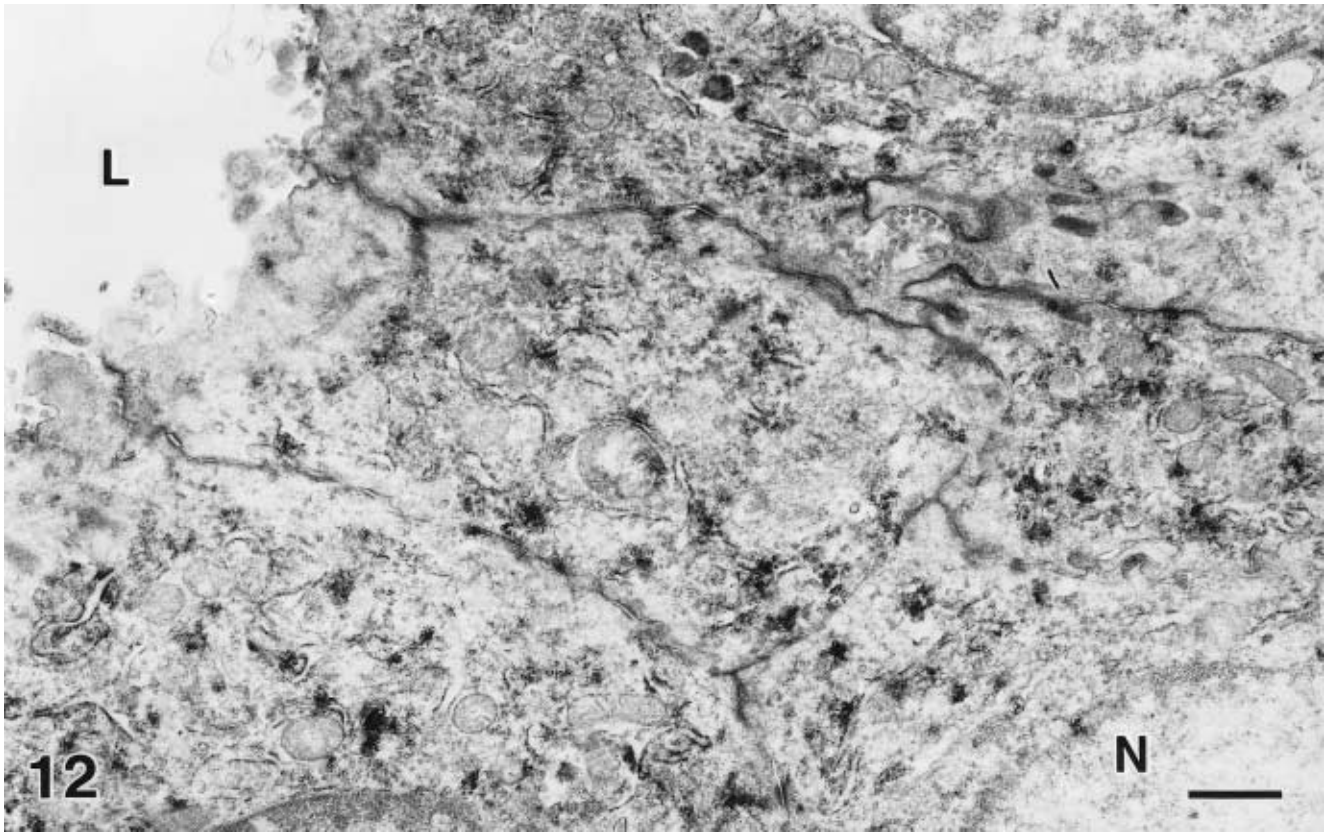

Fig. 12. Immunoelectron photomicrograph of a proliferating biliary epithelial cell at day 7 after CBD ligation. Section incubated with anti-TGF-β_1. The reaction products for TGF-β_1 are predominantly localized on the rough-surfaced endoplasmic reticulum of the biliary epithelial cells. *N*, nucleus, *L*, lumen of bile duct. *Bar* 1 μm

for critical reading of the manuscript, Masatoshi Shirota for expert photographic assistance, and Takako Kadota and Hiroko Yamamoto for secretarial assistance. This study was supported by a Grant-in-Aid for Scientific Research from The Ministry of Education, Science, Sports and Culture in Japan, grants B-09045082 and C-10670162.

References

1. Friedman SL (1993) Seminars in medicine of the Beth Israel Hospital, Boston. The cellular basis of hepatic fibrosis. Mechanisms and treatment strategies. N Engl J Med 328:1828–1835
2. Bissell DM, Friedman SL, Maher JJ, Roll FJ (1990) Connective tissue biology and hepatic fibrosis: report of a conference. Hepatology 11:488–498
3. Ueno T, Sakamoto M, Torimura T, Inuzuka S, Harada M, Yoshitake M, Sakisaka S, Sata M, Yoshida H, Tanikawa K (1990) Morphological changes of sinusoidal cells such as sinusoidal endothelia and the Disse spaces in the process of the hepatic sinusoidal capillarization in man (abstract in English). Med Electron Microsc (formerly J Clin Electron Microsc) 23(3):277–289
4. Ramadori G (1991) The stellate cells (Ito-cell, fat-storing cell, lipocyte, perisinusoidal cell) of the liver. Virchows Arch B Cell Pathol 61:147–158
5. Tanaka Y, Nouchi T, Yamane M, Irie T, Miyakawa H, Sato C, Marumo F (1991) Phenotypic modulation in lipocytes in experimental liver fibrosis. J Pathol 164:273–278
6. Rockey DC, Boyles JK, Gabbiani G, Friedman SL (1992) Rat hepatic lipocytes express smooth muscle actin upon activation in vivo and in culture. J Submicrosc Cytol Pathol 24:193–203
7. Hines JE, Johnson SJ, Burt AD (1993) In vivo responses of macrophages and perisinusoidal cells to cholestatic liver injury. Am J Pathol 142:511–518
8. Enzan H, Himeno H, Iwamura S, Saibara T, Onishi S, Yamamoto Y, Hara H (1994) Immunohistochemical identification of Ito cells and their myofibroblastic transformation in adult human liver. Virchows Arch 424:249–256
9. Gressner AM (1996) Transdifferentiation of hepatic stellate cells (Ito cells) to myofibroblasts: a key event in hepatic fibrogenesis. Kidney Int 49:s39–s45
10. Hautekeete ML, Geerts A (1997) The hepatic stellate (Ito) cell: its role in human liver disease. Virchows Arch 430:195–207
11. Gressner AM, Lotfi S, Gressner G, Lahme B (1992) Identification and partial characterization of a hepatocyte-derived factor promoting proliferation of cultured fat-storing cells (parasinusoidal lipocytes). Hepatology 16:1250–1266
12. Friedman SL (1999) Cytokines and fibrogenesis. Semin Liver Dis 19:129–140
13. Tsukamoto H (1999) Cytokine regulation of hepatic stellate cells in liver fibrosis. Alcohol Clin Exp Res 23:911–916
14. Nakatsukasa H, Evarts RP, Hsia C-C, Thorgeirsson SS (1990) Transforming growth factor-β_1 and type I procollagen transcripts during regeneration and early fibrosis of rat liver. Lab Invest 63:171–180
15. Milani S, Herbst H, Schuppan D, Stein H, Surrenti C (1991) Transforming growth factors β_1 and β_2 are differentially expressed in fibrotic liver disease. Am J Pathol 139:1221–1229
16. Bissell DM, Wang SS, Jarnagin WR, Roll FJ (1995) Cell-specific expression of transforming growth factor-β in rat liver. Evidence for autocrine regulation of hepatocyte proliferation. J Clin Invest 96:447–455
17. Maher JJ, McGuire RF (1990) Extracellular matrix gene expression increases preferentially in rat lipocytes and sinusoidal

endothelial cells during hepatic fibrosis in vivo. J Clin Invest 86:1641–1648
18. Aronson DC, De Haan J, James J, Bosch KS, Ketel AG, Houtkooper JM, Heijmans HSA (1988) Quantitative aspects of the parenchyma-stroma relationship in experimentally induced cholestasis. Liver 8:116–126
19. Abdel-Aziz G, Lebeau G, Rescan P-Y, Clément B, Rissel M, Deugnier Y, Campion J-P, Guillouzo A (1990) Reversibility of hepatic fibrosis in experimentally induced cholestasis in rat. Am J Pathol 137:1333–1342
20. Hinz S, Franke H, Machnik G, Müller A, Dargel R (1997) Histological and biochemical changes induced by total bile duct ligation in the rat. Exp Toxic Pathol 49:281–288
21. Abdel-Aziz G, Rescan P-Y, Clement B, Lebeau G, Rissel M, Grimaud J-A, Campion J-P, Guillouzo A (1991) Cellular sources of matrix proteins in experimentally induced cholestatic rat liver. J Pathol 164:167–174
22. Housset C (2000) Biliary epithelial cell response to cholestasis. J Hepatol 32 (suppl 2):14–15
23. Kinnman N, Hultcrantz R, Barbu V, Rey C, Wendum D, Poupon R, Housset C (2000) PDGF-mediated chemoattraction of hepatic stellate cells by bile duct segments in cholestatic liver injury. Lab Invest 80:697–707
24. Saito JM, Maher JJ (2000) Bile duct ligation in rats induces biliary expression of cytokine-induced neutrophil chemoattractant. Gastroenterology 118:1157–1168
25. Miyazaki H, Van Eyken P, Roskams T, De Vos R, Desmet VJ (1993) Transient expression of tenascin in experimentally induced cholestatic fibrosis in rat liver: an immunohistochemical study. J Hepatol 19:353–366
26. Tang L, Tanaka Y, Marumo F, Sato C (1994) Phenotypic change in portal fibroblasts in biliary fibrosis. Liver 14:76–82
27. Tuchweber B, Desmoulière A, Bochaton-Piallat ML, Rubbia-Brandt L, Gabbiani G (1996) Proliferation and phenotypic modulation of portal fibroblasts in the early stages of cholestatic fibrosis in the rat. Lab Invest 74:265–278
28. Desmoulière A, Darby I, Costa AMA, Raccurt M, Tuchweber B, Sommer P, Gabbiani G (1997) Extracellular matrix deposition, lysyl oxidase expression, and myofibroblastic differentiation during the initial stages of cholestatic fibrosis in the rat. Lab Invest 76:765–778
29. Kountouras J, Billing BH, Scheuer PJ (1984) Prolonged bile duct obstruction: a new experimental model for cirrhosis in the rat. Br J Exp Pathol 65:305–311
30. Enzan H, Hayashi Y, Miyazaki E, Naruse K, Tao R, Kuroda N, Nakayama H, Kiyoku H, Hiroi M, Saibara T (1999) Morphological aspects of hepatic fibrosis and Ito cells (hepatic stellate cells), with special reference to their myofibroblastic transformation. In: Tanikawa K, Ueno T (eds) Liver diseases and hepatic sinusoidal cells. Springer, Tokyo, pp 219–231
31. Niiro G, O'Morchoe CC (1986) Pattern and distribution of intrahepatic lymph vessels in the rat. Anat Rec 215:351–360
32. Bronfenmajer S, Schaffner F, Popper H (1966) Fat-storing cells (lipocytes) in human liver. Arch Pathol 82:447–453
33. Grinko I, Geerts A, Wisse E (1995) Experimental biliary fibrosis correlates with increased numbers of fat-storing and Kupffer cells, and portal endotoxemia. J Hepatol 23:449–458
34. Ramm GA, Nair VG, Bridle KR, Shepherd RW, Crawford DH (1998) Contribution of hepatic parenchymal and nonparenchymal cells to hepatic fibrogenesis in biliary atresia. Am J Pathol 153:527–535
35. Saperstein LA, Jirtle RL, Farouk M, Thompson HJ, Chung KS, Meyers WC (1994) Transforming growth factor-β_1 and mannose 6-phosphate/insulin-like growth factor-II receptor expression during intrahepatic bile duct hyperplasia and biliary fibrosis in the rat. Hepatology 19:412–417
36. Marra F, Romanelli RG, Giannini C, Failli P, Pastacaldi S, Arrighi MC, Pinzani M, Laffi G, Montalto P, Gentilini P (1999) Monocyte chemotactic protein-1 as a chemoattractant for human hepatic stellate cells. Hepatology 29:140–148
37. Pinzani M, Gentilini A, Caligiuri A, De Franco R, Pellegrini G, Milani S, Marra F, Gentilini P (1995) Transforming growth factor-β_1 regulates platelet-derived growth factor receptor β subunit in human liver fat-storing cells. Hepatology 21:232–239